

# The p.P1127S pathogenic variant lowers von Willebrand factor levels through higher affinity for the macrophagic scavenger receptor LRP1: Clinical phenotype and pathogenic mechanisms

Monica Sacco<sup>1</sup>  | Stefano Lancellotti<sup>2</sup> | Alessio Branchini<sup>3</sup>  | Maira Tardugno<sup>1</sup> |  
 Maria Francesca Testa<sup>3</sup> | Barbara Lunghi<sup>3</sup> | Francesco Bernardi<sup>3</sup> | Mirko Pinotti<sup>3</sup> |  
 Betti Giusti<sup>4,5</sup> | Giancarlo Castaman<sup>6</sup> | Raimondo De Cristofaro<sup>1,2</sup> 

<sup>1</sup>Dipartimento di Medicina e Chirurgia  
 Traslationale, Facoltà di Medicina e  
 Chirurgia "Agostino Gemelli," Università  
 Cattolica S. Cuore, Roma, Italy

<sup>2</sup>Servizio Malattie Emorragiche e  
 Trombotiche, Fondazione Policlinico  
 Universitario "A. Gemelli" IRCCS, Roma, Italy

<sup>3</sup>Dipartimento di Scienze della Vita e  
 Biotecnologie, Università di Ferrara,  
 Ferrara, Italy

<sup>4</sup>Dipartimento di Medicina Sperimentale e  
 Clinica, Università di Firenze, Firenze, Italy

<sup>5</sup>Laboratorio Genetico Molecolare  
 Avanzato, SOD Malattie  
 Aterotrombotiche, Azienda Ospedaliero-  
 Universitaria "Careggi", Firenze, Italy

<sup>6</sup>Dipartimento di Oncologia, Centro  
 Malattie Emorragiche e della  
 Coagulazione, Ospedale Universitario  
 "Careggi", Firenze, Italy

## Correspondence

Raimondo De Cristofaro, Dipartimento  
 di Medicina e Chirurgia Traslationale,  
 Facoltà di Medicina e Chirurgia "Agostino  
 Gemelli", Università Cattolica S. Cuore,  
 Roma, Italy. Fondazione Policlinico  
 Universitario "A. Gemelli" IRCCS,  
 Largo A. Gemelli 8, 00168 Roma, Italy.  
 Email: [raimondo.decrisofaro@unicatt.it](mailto:raimondo.decrisofaro@unicatt.it)

## Funding information

Università Cattolica del Sacro Cuore  
 - ROMA, Grant/Award Number: Grant  
 "Linea D1-2019"

## Abstract

**Background:** The index case is a 21-year-old Italian woman with a mild hemorrhagic syndrome and von Willebrand factor antigen (VWF:Ag) = 34.3 U/dl, VWF recombinant glycoprotein Ib (VWF:GpIbR) = 32.8 U/dl, and factor VIII (FVIII) = 55.3 IU/dl.

**Aims:** The aim of this study is to characterize from a genetic and biochemical standpoint this low VWF phenotype.

**Methods:** Coagulation and biochemical methods were used to study the structural and functional pattern of VWF multimers in the index case's plasma. Recombinant wild-type and p.P1127S VWF variants were produced using human embryonic kidney (HEK)-293 cells. In addition, genetic screening was carried out to detect single nucleotide variants of some scavenger VWF/FVIII receptor genes such as *CLEC4M*, *STAB2*, and *ASGR2*.

**Results:** Genetic investigation revealed that the index case inherited from her mother the heterozygous missense mutation c.3379C>T (VWF exon 25), causing the p.P1127S substitution in the VWF D'D3 domain. The index case was also homozygous for the scavenger receptor ASGR2 c.-95 CC-genotype. Desmopressin normalized the VWF level of the patient, although its clearance was faster ( $t_{1/2} = 6.7$  h) than in normal subjects ( $t_{1/2} = 12 \pm 0.7$  h). FVIII-VWF interaction, A Disintegrin And Metalloprotease with ThromboSpondin type 1 motif-13 levels, ristocetin-induced-platelet-aggregation, and VWF multimeric pattern were normal. The p.P1127S variant was normally synthesized and secreted by HEK-293 cells, and molecular modeling predicts a conformational change showing higher affinity for the macrophagic scavenger receptor lipoprotein receptor-related protein 1 (LRP1), as also experimentally verified.

Monica Sacco and Stefano Lancellotti contributed equally to this study.

Giancarlo Castaman and Raimondo De Cristofaro are co-senior authors.

Manuscript handled by: David Lillicrap, 17-May-2022

Final decision: David Lillicrap

This is an open access article under the terms of the [Creative Commons Attribution-NonCommercial-NoDerivs](https://creativecommons.org/licenses/by-nc-nd/4.0/) License, which permits use and distribution in any medium, provided the original work is properly cited, the use is non-commercial and no modifications or adaptations are made.

© 2022 The Authors. *Journal of Thrombosis and Haemostasis* published by Wiley Periodicals LLC on behalf of International Society on Thrombosis and Haemostasis.

**Conclusions:** The p.P1127S variant may cause a low VWF phenotype, stemming from an increased VWF affinity for the scavenger receptor LRP1 and, consequently, an accelerated clearance of VWF.

**KEYWORDS**

asialoglycoprotein receptor 2, lipoprotein receptor-related protein 1, protein conformation, scavenger receptors, von Willebrand disease, von Willebrand factor

## 1 | INTRODUCTION

Von Willebrand factor (VWF) is a large multimeric glycoprotein that mediates platelet adhesion to the damaged vessel wall under high shear stress conditions, serving also as carrier for factor VIII (FVIII), an essential cofactor for the generation of activated factor X (FX).<sup>1</sup> The VWF gene, localized on chromosome 12, spans 178 kb and contains 52 exons. The VWF mature subunit is composed of four repetitive domains designated A to D and arranged in the sequence D'-D3-A1-A2-A3-D4-C1-C2-C3-C4-C5-C6-CK.<sup>2-5</sup> The von Willebrand disease (VWD) is the most common inherited bleeding disorder in humans, is largely heterogeneous, and is characterized by quantitative and/or qualitative defects of VWF.<sup>5</sup> The classification of congenital VWD is based on both clinical and laboratory findings according to recently published recommendations.<sup>6-8</sup> Type 1 VWD differentiates from the type 2 forms, as it causes only quantitative defects of VWF while the latter shows qualitative/quantitative VWF abnormalities.<sup>9</sup> Finally, type 3 VWD is characterized by complete absence of circulating VWF multimers. Type 1 VWD may be difficult to identify due to a variety of pathogenic mechanisms involved and should be diagnosed only in the presence of VWF levels  $\leq 30$  IU/dl and significant bleeding phenotypes.<sup>8</sup> The patients with type 1 VWD are likely to carry identifiable VWF gene mutations, exhibiting autosomal dominant inheritance patterns.<sup>8,10</sup> At variance, the patients with slightly reduced VWF levels between 30 and 50 IU/dl should be considered in a separate category labeled "low VWF levels."<sup>11</sup> These patients commonly display variable bleeding manifestations and often do not have VWF gene sequence variations. Among type 1 VWD forms, the subtype referred to as 1C is characterized by the increased clearance of VWF molecules and is associated with gene mutations in different VWF domains.<sup>12,13</sup> Whereas several mutations are located in the D3 domain, missense mutations affecting the A1 domain were shown to significantly enhance VWF clearance in type 2B VWD via a low-density lipoprotein receptor-related protein 1 (LRP1)-dependent mechanism.<sup>14</sup> Further studies will be required to define the molecular mechanisms through which different mutations may lead to increased VWF clearance, and rare missense variants could contribute to mild phenotypes. Clinical evaluation is difficult because: (1) many patients present nonspecific mild bleeding symptoms as moderately low VWF levels (30–50 IU/dl) are weak risk factors for bleeding; (2) subjects with type "O" blood group show VWF levels 30–40% lower than those observed in the other blood groups and; finally, (3) low VWF levels are characterized by low heritability. Moreover, bleeding

### Essentials

- A 21-year-old girl with a mild hemorrhage had low von Willebrand factor (VWF) levels and the heterozygous pathogenic variant *c.C3379 > T*.
- This pathogenic variant caused the p.P1127S substitution in the VWF D'D3 domain.
- The patient also carried the homozygous *c.-95 CC* single nucleotide polymorphism of asialoglycoprotein receptor 2, one of the factor VIII/VWF scavengers.
- These genetic mutations change the VWF conformation, accelerates its clearance, and cause a low VWF disease.

and low VWF levels associate in many patients only by chance. A variety of cell surface receptors has been found to bind with high affinity to the FVIII/VWF complex, modulating the residency time of these factors in circulation.<sup>15</sup> These cell receptors include the low-density-lipoprotein receptor (LDLR),<sup>16</sup> C-type lectin domain family 4 member M (CLEC4M),<sup>17</sup> stabilin-2 (STAB2),<sup>18</sup> LRP1,<sup>19</sup> and the asialoglycoprotein receptor (ASGPR),<sup>20</sup> part of which bind with high affinity to VWF/FVIII molecules through their N-linked oligosaccharide structures.<sup>20,21</sup> With this background, we aimed to unravel the molecular pathogenesis of a mild hemorrhagic tendency in an index case with low VWF level. Hence, a genetic and biochemical examination was carried out to assess whether possible pathogenic VWF variants or single nucleotide variants (SNVs) of the above-mentioned scavenger cell receptors could determine the phenotype. The index case was investigated by complementary strategies based on analysis of clinical data, phenotype, gene sequencing, recombinant expression studies, and molecular modeling of the mutated VWF molecule.

## 2 | MATERIALS AND METHODS

### 2.1 | Patient

The index case, a 21-year-old Italian girl, showed a vast hematoma of the right thigh appearing after a modest trauma. The Bleeding Score System (BSS) was equal to 3 (menorrhagia 1, hematoma 2). She declared to suffer from minor bruising after assumption of non-steroid-anti-inflammatory drugs, although she did not suffer heavy

menstrual bleeding. No chronic disease was reported in the anamnesis of the patient. The father of the index case suffered from rectorrhagia due to the presence of rectal polyps. The mother of the patient was also studied from a genetic and phenotypic standpoint. She reported to have had heavy menstrual bleeding in the fertile age. In addition, she had had epistaxis events (about 1 event/month) up to age 30 (BSS = 2), when these phenomena ceased. The main laboratory parameters of the index case and her mother are listed in Table 1. A signed informed consent was given by the family members, according to the Declaration of Helsinki.

## 2.2 | Measurements of VWF-related parameters

VWF-antigen (VWF:Ag) and VWF activity (measured as binding capacity to glycoprotein Ib [Gplb], VWF:GplbR) were measured by chemiluminescence assays (ACL Acustar, Instrumentation Laboratory, Werfen Group).<sup>22,23</sup> VWF-collagen binding assay (CBA) was performed using the Asserachrom® VWF:CBA (Stago). VWFpp was measured by an ELISA assay (Sanquin), as previously detailed.<sup>12</sup> FVIII-VWF interaction was studied with the commercially available Asserachrom®VWF:VIII assay (Stago).<sup>24</sup> FVIII activity was measured using a chromogenic assay (Instrumentation Laboratory, Werfen Group). Activity of A

Disintegrin And Metalloprotease with ThromboSpondin type 1 motif-13 (ADAMTS-13) was measured by a fluorescence resonance energy transfer assay, as previously detailed.<sup>25</sup>

## 2.3 | Electrophoresis of VWF multimers

VWF multimeric pattern was studied with low- (0.8–1.5% agarose, LR-SDS-AGE [low-resolution sodium dodecyl sulfate agarose gel electrophoresis]) and high-resolution (0.8–2.5%) SDS-AGE (HR-SDS-AGE), as previously reported.<sup>26</sup> Proteolyzed VWF products formed by recombinant ADAMTS-13 were analyzed by western blotting using gradient 4–12% SDS polyacrylamide gel electrophoresis (SDS-PAGE) gels, as previously detailed.<sup>27</sup>

## 2.4 | Molecular genetics of VWF

A bidirectional direct sequencing of polymerase chain reaction (PCR) products by direct sequencing of exons 1 to 52, including exon/intron boundaries, 5' and 3' untranslated region, was performed with an ABI 3500Dx Sequencer (Applied Biosystems), as previously detailed.<sup>28</sup> The paternity test was performed with the Power-Plex-16

TABLE 1 Laboratory parameters of the index case and her mother

Parameter	Index case	Index case Post-DDAVP(1 h)	Mother	Normal values
Gene mutations	Heterozygous polymorphic c.C3379 > T (exon 25) → (p.P1127S)		Heterozygous polymorphic c.C3379 > T (exon 25) → (p.P1127S)	
Age	21	21	54	
INR	0.96	0.95	0.95	0.8–1.2
APTT (s)	35.8	31.1	34.5	22–37
Fibrinogen (mg/dl)	326	338	316	200–400
VWF:Ag (IU/dl)	34.3	84	57.1	50–150
VWF:GplbR (IU/dl)	32.8	80	63.1	50–150
VWF:CBA (IU/dl)	33	ND	58.3	50–150
FVIII (IU/dl)	55.3	123	72.4	50–150
VWFpp (%)	43	127	52.1	50–120
VWF:GplbR/VWF:Ag	0.96	0.95	1.1	0.75–1.25
VWF:CBA/VWF:Ag	0.96	ND	1.1	0.75–1.2
VWFpp/VWF:Ag	1.30	1.52	0.91	0.75–1.25
FVIII/VWF:Ag	1.61	1.07	1.3	0.75–1.25
FVIII-VWF binding (%)	95	ND	80.7	70–130
ADAMTS-13 act (%)	84.1	ND	92.2	70–130
Platelets (×10 <sup>9</sup> /L)	313	265	189	200–400
Hb (g/dl)	12.8	13.4	13.1	12.5–15
Blood group	A1-Rh+	-	O-Rh+	-

Abbreviations: ADAMTS-13, A Disintegrin And Metalloprotease with ThromboSpondin type 1 motif-13; Ag, antigen; APTT, activated partial thromboplastin time; CBA, collagen binding assay; FVIII, factor VIII; Gplb, glycoprotein b; Hb, hemoglobin; INR, international normalized ratio; ND, not determined; VWF, von Willebrand factor.

kit (Promega Corp.) following the manufacturer's instructions. Analysis of the PCR products (3  $\mu$ l) was carried out with the 3100-Avant Genetic Analyzer (Applied Biosystems). The quality control followed the proficiency testing of International Society for Forensic Genetics Working Group guidelines.<sup>29</sup>

## 2.5 | Molecular genetics of VWF receptors

The SNVs of ASGR2 (rs2289645 T>C), CLEC4M (rs868875 A>G), LDLR (rs688 C>T), and STAB2 (rs4981022 A>G) were detected by PCR and restriction. Table S1 reports the details of VWF receptor gene variants investigated in the index case and her mother. The A2 allele of the ABO blood group was investigated as previously described.<sup>30</sup>

## 2.6 | In vitro expression of recombinant WT and p.P1127S VWF variants

The p.P1127S missense pathological variant was inserted by site-directed mutagenesis (QuickChange® II XL Site-Directed Mutagenesis Kit, Agilent Technologies) of the VWD cDNA (reference sequence NM\_000552), cloned in the pCDNA3 expression vector, using the 5' GC CACATTGTGCTCCCAGAGCTGCG 3' (forward) and 5' CGCAGCTCTGGAGCACAATGTGGC 3' (reverse) oligonucleotides (modified nucleotide underlined). The plasmid was validated by sequencing.

Human embryonic kidney (HEK)-293 cells were used for expression studies. Cell culture, transient transfection, and VWF purification were performed as previously described.<sup>28</sup>

## 2.7 | Platelet aggregation studies

Platelet aggregation studies were performed in platelet-rich plasma with an AggRAM platelet aggregometer (Helena Biosciences) using 2–10  $\mu$ M ADP, 10  $\mu$ g/ml collagen, and 0.15–1.2 mg/ml ristocetin (Helena Biosciences). The recombinant wild-type (WT)-VWF, heterozygous, and homozygous p.P1127S VWF constructs were tested with normal platelets (200000 plt/ $\mu$ l) of a healthy donor in platelet aggregation studies using 1.2, 0.4, and 0.2 mg/ml (final concentrations) ristocetin in 10 mM HEPES-buffered saline, pH 7.40. The final concentration of each VWF construct was set at 20 U/dl.

## 2.8 | DDAVP test

Intravenous infusions of 1-Desamino-8-D-arginine vasopressin (desmopressin, DDAVP dose: 0.3  $\mu$ g/kg body weight, diluted in 100 ml saline) were given under medical supervision. Blood was withdrawn for VWF/FVIII analysis at baseline and 1, 3, 5, 6, 8 h after the infusion end. The pharmacokinetics of VWF levels after desmopressin infusion was investigated by the WinNonlin program (Certara University), according to a non-compartmental analysis for intravenous infusion.

## 2.9 | Binding of WT- and p.P1127S-VWF mutant to immobilized LRP1

Bovine serum albumin (BSA; 2  $\mu$ g/ml) or human rLRP1-cIV/Fc (R&D) was adsorbed overnight to microtiter wells at 2  $\mu$ g/ml in 50 mM Na<sub>2</sub>CO<sub>3</sub> and 10 mM NaHCO<sub>3</sub>, pH 9.6 at 4°C. To avoid non-specific binding, blocking buffer (Tris-buffered saline supplemented with 0.1% Tween-20, 5% BSA, and 5 mM CaCl<sub>2</sub>) was used for 2 h at 37°C. Wells were subsequently incubated with different concentrations of both WT and p.P1127S-VWF mutant over a concentration range of 0–20 nM, diluted in 200  $\mu$ l blocking buffer also containing 1 mg/ml ristocetin in the absence or presence of 5 mM ethylenediaminetetraacetic acid for 2 h at 37°C. Bound VWF was probed with polyclonal rabbit anti-human VWF and a fluorescein isothiocyanate-conjugated swine anti-rabbit IgG secondary antibody (both from Dako) diluted 1:50 in blocking buffer for 2 h at 37°C.

## 2.10 | Proteolysis in vitro of recombinant VWF constructs by ADAMTS-13

Proteolysis of 16 IU/dl WT, heterozygous, and homozygous p.P1127S recombinant forms was studied using 2.5 nM recombinant human ADAMTS-13 (R&D) in a solution containing 20 mM CHES/10 mM BisTris/10 mM Tris, 2.5  $\mu$ M ZnCl<sub>2</sub>, and 5 mM CaCl<sub>2</sub>, pH 7.40 at 25°C. The reaction was stopped with sample buffer at 1, 3, 5, and 8 h and the products analyzed by western blotting.

## 2.11 | In silico modeling of the missense VWF p.P1127S mutant monomer and interaction with LRP1

The heterozygous p.P1127S pathogenic variant identified in the VWF molecule found in the patient and her mother is localized in the D'D3 domain, whose X-ray structures have only been partly resolved. X-ray crystal VWF structures deposited in the Protein Data Bank (PDB) website are the D'D3 (S764-P1241, PDB file ID "6N29"), A1 (D1261-1468, PDB file ID "1AUQ"), A2 (M1495-H1674, PDB file ID "3GXB"), and A3 domains (D1685-S1873, PDB file ID "1ATZ"). Thus, we used the above X-ray-solved structures as partial templates, performing a molecular modeling of the remaining sequences of the entire VWF region S764-V2191. This analysis was carried out using the I-TASSER threading modeling server (Iterative ThreadingASSEMBLY Refinement; <http://zhanglab.cmb.med.umich.edu/I-TASSER/>), as previously detailed.<sup>28</sup> The interaction between the models of both WT and the homozygous-p.P1127S VWF mutant with the extracellular domain (cluster IV) of LRP1 (residues 3331–3780)<sup>19</sup> was investigated *in silico* using the SwarmDock platform (<https://bmm.crick.ac.uk/~svc-bmm-swarmdock/submit.cgi>) and in some cases the ClusPro program to compare and confirm the data.<sup>31</sup> The 3331–3780 region of LRP1, which regulates VWF and other ligands' binding, was modeled by using the I-TASSER server.

### 3 | RESULTS

#### 3.1 | VWF-related parameters

The index case showed similar reduction of VWF:Ag, VWF:GpIbR, and VWF:CBA levels, as listed in Table 1. These findings agreed with the multimer VWF analysis that showed a normal presence of all components of any molecular weight in SDS-AGE, as shown in Figure 1. The FVIII activity was in the lower normal range with a FVIII/VWF ratio = 1.61. No defect of FVIII binding to VWF was observed, being equal to 95% and 80.7% in the index case and her mother (Table 1). In the index case, the VWFpp/VWF:Ag ratio resulted slightly increased (1.3),<sup>12</sup> whereas it was normal in her mother (Table 1). After the desmopressin infusion, the VWFpp/VWF:Ag ratio in the index case increased to 1.52.

#### 3.2 | Platelet aggregation

The patient and her mother showed a normal platelet aggregation by ADP (maximal aggregation = 89% and 94%, respectively), collagen (maximal aggregation = 98% and 100%, respectively), and 1.2 mg/ml ristocetin (maximal aggregation = 75% and 93%, respectively). At 0.6 mg/ml ristocetin, maximal aggregation ruled out the presence of type 2B VWD, being in both cases equal to 3% (index case) and 5% (mother). The recombinant VWF constructs, rVWF-WT, heterozygous p.P1127S, and homozygous

p.P1127S in radioimmunoprecipitation assay showed similar aggregation response at any ristocetin concentration used (1.2, 0.4, and 0.2 mg/ml), as shown in Figure S1.

#### 3.3 | DDAVP test

The index case and her mother showed a good response to desmopressin. However, the kinetic profile (PK) of VWF level after desmopressin infusion in the index case showed an accelerated phase of clearance (Figure 2). The first-order kinetics concerning the decrease of VWF value in the patient was faster ( $t_{1/2} = 6.7$  h) than in three normal subjects bearing the same type A blood group ( $t_{1/2} = 12 \pm 0.7$  h). The VWF:pp/VWF:Ag ratio of the index case did not significantly change after desmopressin infusion (1.3 at baseline, 1.52 after 1 h, and back to 1.28 after 8 h), although the values were in the upper limits of a normal range. The mother showed an intermediate  $t_{1/2}$  value, being equal to 9.6 h, as shown in Figure 2. The complete results of the PK analysis of all subjects are reported in Figure S2A–E.

#### 3.4 | Characterization of the VWF genetic mutation

Sequencing of the VWF gene revealed a single sequence variant in both the patient and her mother, the heterozygous c.3379C>T mutation. The genetic variant c.3379C>T identified in exon 25 of the VWF gene causes the p.P1127S substitution in the D'D3 domain of

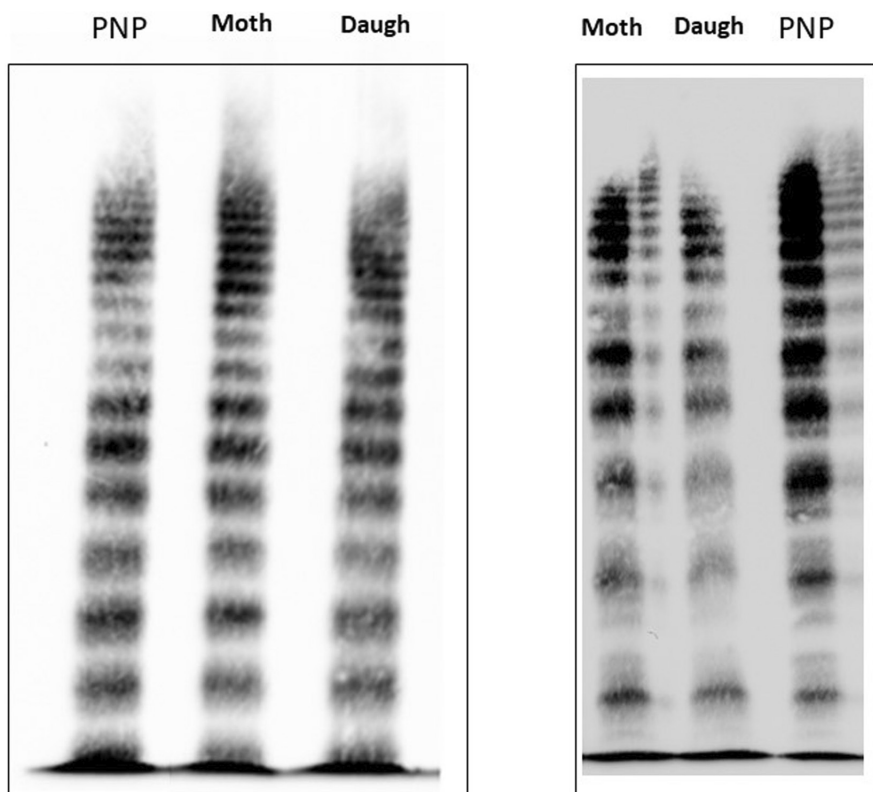


**FIGURE 1** Von Willebrand factor (VWF) multimers pattern of the index case, her mother (Moth) and pooled normal plasma (PNP). In low-resolution (LR)-sodium dodecyl sulfate (SDS)-agarose gel electrophoresis (AGE; left) all the components of VWF multimers are present. In high-resolution (HR)-SDS-AGE the multimeric pattern with the “triplet” sub-bands are also shown.

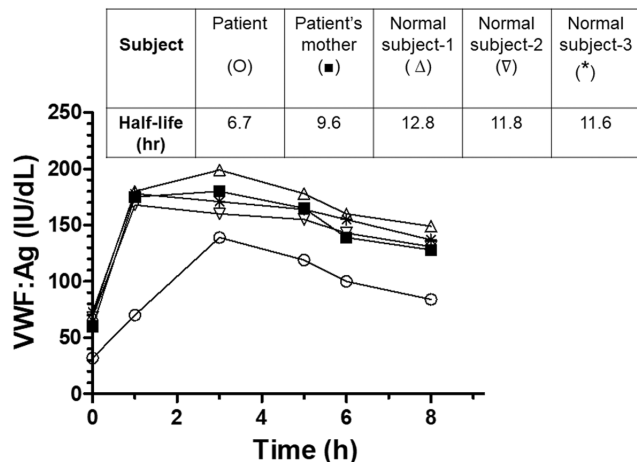


**FIGURE 2** Pharmacokinetic profile of von Willebrand factor antigen (VWF:Ag) levels after intravenous (i.v.) infusion of desmopressin at a dose of 0.3  $\mu\text{g}/\text{kg}$ . O Patient, mother of the index case, while ■, ∇, and \* refer to three normal subjects characterized by baseline VWF levels comparable to that of the patient's mother. The calculated  $t_{1/2}$  values of VWF clearance are listed in the inset table. The pharmacokinetic analysis was performed using the WinNonlin program employing a non-compartmental and i.v. infusion model.

the mature molecule. This variant is reported in the dbSNP database, rs139579968, with a minor allele frequency in the European population between 0.0001 and 0.0004 (<http://www.ncbi.nlm.nih.gov/snp/>). Forty alleles are also reported in gnomAD ([https://gnomad.broadinstitute.org/variant/12-6023631-G-A?dataset=gnomad\\_r3](https://gnomad.broadinstitute.org/variant/12-6023631-G-A?dataset=gnomad_r3)). The father of the index case did not show this mutation, and his paternity was confirmed by a paternity assay resulting in a Combined Paternity Index (CPI)  $>299 \times 10^6$  and a paternity probability  $>99.99999\%$ . PolyPhen-2 (<http://genetics.bwh.harvard.edu/pph2/>) and SIFT (<https://sift.bii.a-star.edu.sg/>) suggested that this variant may be damaging to protein expression and/or function. Likewise, both the Combined Annotation Dependent Deletion (CADD) and Rare Exome Variant Ensemble Learner (REVEL) scores revealed a deleterious effect of the pathogenic variant ([http://www.ensembl.org/Homo\\_sapiens/Variation/Mappings?db=core;r=12:60231-31-6024131;v=rs139579968;vdb=variation;vf=194601477](http://www.ensembl.org/Homo_sapiens/Variation/Mappings?db=core;r=12:60231-31-6024131;v=rs139579968;vdb=variation;vf=194601477)). CADD score was indeed equal to 33 (likely deleterious) and the REVEL score was equal to 0.748 (likely disease-causing).

### 3.5 | VWF/FVIII receptors genotypes

Several receptors have been experimentally implicated in VWF/FVIII clearance and half-life both in hemophilic patients and in animal models.<sup>15–18,20,21</sup> Based on this hypothesis, we have investigated the possible presence of known SNVs (Table S1) of scavenger receptors in the index case and her mother. Identical genotypes were found (CLEC4M rs868875 A>G, LDLR rs688 C>T, and STAB2 rs4981022 A>G) except for the ASGR2 rs2289645 T>C SNVs. Whereas the index case was homozygous for the non-reference C

allele, her mother was heterozygous. The A2 blood group that determines VWF levels very similar to those observed in the O group<sup>30</sup> was not detected in the family.

### 3.6 | Expression of WT and p.P1127S VWF mutant

The synthesis and expression level of the p.P1127S variant was found normal in the medium and HEK-293 cell lysates, as shown in Figure 3A. The SDS-PAGE showed a normal profile of VWF multimers, as shown in Figure 3B. This finding shows that the p.P1127S VWF variant is normally synthesized and secreted.

### 3.7 | In vitro proteolysis of recombinant VWF constructs by ADAMTS-13

Both the heterozygous and homozygous constructs did not show in SDS-PAGE and western blotting analysis an abnormal proteolysis at any time point of the reaction, compared to the WT form (see for instance the proteolyzed fragments obtained after 8 h since the beginning of the reaction in Figure S3). This finding agreed with the multimeric profile observed for plasma VWF of the patient and her mother by low- and high-resolution SDS-AGE (see Figure 1), not showing abnormalities in multimer composition and triplet sub-bands, respectively.

### 3.8 | Molecular modeling of the missense pathogenic variant p.P1127S

I-TASSER was used to generate structure predictions for both the WT VWF monomer and mutant bearing the p.P1127S pathogenic variant (sequence 764–2191). The template modeling score of the predicted model was found equal to  $0.75 \pm 0.1$  for the WT model and  $0.73 \pm 0.11$  for the P1127S mutant. The comparative structural analysis of the best models of the 764–2191 sequence of both the WT and mutant form showed a root mean squared distance value = 41.8. This reflects a large difference in the 3D configuration of the sequences that differ only by a single amino acid (Pro1127 vs. Ser1127), as shown in Figure 4A,B. Notably, the region spanning from Glu950 to Ser1028 assumes a different tertiary conformation compared to the predicted WT-VWF construct (Figure 4B), assuming a more open conformation that is more exposed to solvent and likely a higher conformational flexibility. This difference was even more evident when the two models of the WT and the p.P1127S mutant were overlapped and aligned (Figure 4C). Notably, even when the region Gly1115–Arg1133 (containing the residue 1127) was analyzed alone *in silico*, it undergoes significant conformational changes when Pro1127 is mutated to serine (Figure 5). The original, more compact conformation is lost in the mutated peptide region that, becoming a linear random coil, triggers a local rearrangement, which allosterically propagates to long-range distances involving the region spanning from Glu950 to Ser1028 in the VWF monomer.

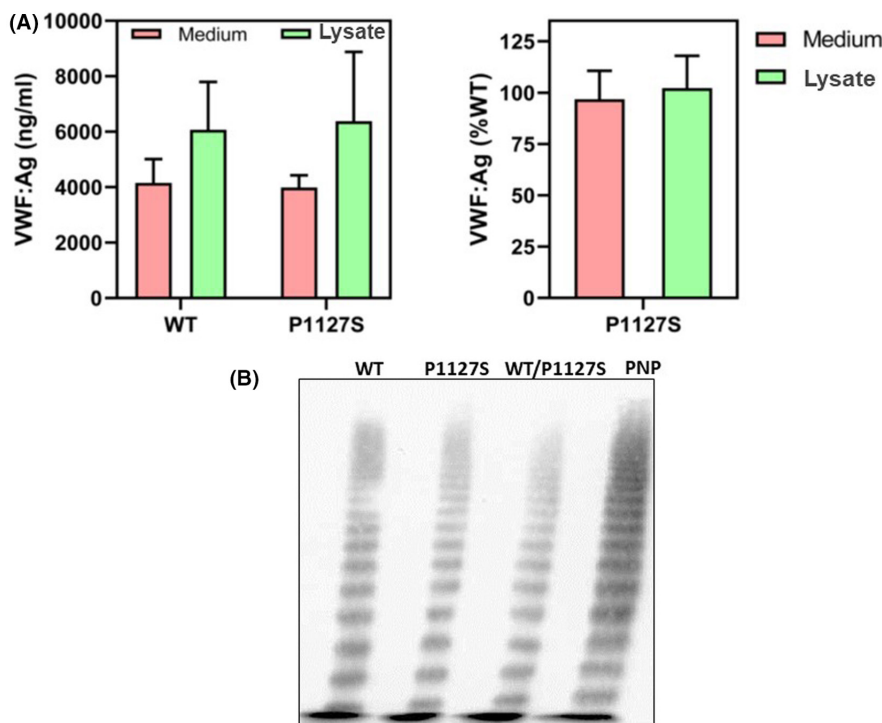


**FIGURE 3** (A) ELISA of recombinant von Willebrand factor antigen (recVWF:Ag) concentration of wild-type (WT) and homozygous p.P1127S in medium and lysate samples from seven replicates in two independent transfections cycles of human embryonic kidney (HEK)-293 cells. On the left, the absolute VWF:Ag values in ng/ml; on the right, values in % of the WT, used as a reference. Similar results were obtained with the heterozygous p.P1127S variant (not shown). Statistical analysis (Mann-Whitney test) showed no significant difference of the VWF:Ag level between the WT and the p.P1127S variant in the medium ( $4152 \pm 864$  ng/ml vs.  $3988 \pm 444$  ng/ml, respectively,  $p = .99$ ) and similarly in the lysate samples ( $6075 \pm 1722$  ng/ml vs  $6376 \pm 2507$  ng/ml, respectively,  $p = .90$ ). On the right, VWF levels of the p.P1127S variant, normalized for the WT levels, did not differ in the lysate samples and in the medium ( $96.8 \pm 13.6\%$  vs.  $102.3 \pm 15.7$ ,  $p = .71$ ). B, Sodium dodecyl sulfate (SDS)-agarose gel electrophoresis gels (agarose = 1.5%) of VWF multimers of recombinant constructs, that are WT, homozygous p.P1127S, and heterozygous p.P1127S mutant. A normal plasma sample (pooled normal plasma [PNP]) was also analyzed as a control.

These conformational changes were further investigated to provide a prediction of their effects on the interaction of VWF with the cluster IV of the extracellular part of LRP1, the main scavenger molecule of VWF, in the attempt to explain, at least in part, the accelerated clearance observed *in vivo* in our patient. The results of the predictive docking experiments are shown in Figure 6A,B. The WT VWF monomer binding involves the amino acid sequences 1359–1362, 1399–1402, 1414–1419, 1486–1492, 2090–2096, 2124–2130. The binding region of the p.P1127S mutant is different, as it involves the sequences 1854–1863, 1868–1871, 1895–1907, 1924–1937, 1948–1960, 1995–2002, 2089–2101, 2178–2179. Even the LRP1 regions engaged in the interaction with the WT and the mutant VWF are different, being involved the 190–300 amino acid sequence for the WT form and the amino terminus 1–40 in the case of the p.1127S mutant. The charged, polar, and apolar contacts between the model of the Cluster IV of human LRP1 and both WT-VWF and p.P1127S pathogenic variant are listed in Table S2. Hence, the energetics of the two interactions, calculated using the Prodigy program,<sup>32</sup> is also different, being characterized by a  $\Delta G = -14.1$  kcal/mol ( $K_d$  at  $25^\circ\text{C} = 4.7 \times 10^{-11}$  M) and  $-15.2$  kcal/mol ( $K_d$  at  $25^\circ\text{C} = 7.3 \times 10^{-12}$

M) for the WT and the p.P1127S variant, respectively. Moreover, considering the prototypic example for an accelerated VWF clearance mediated by the macrophage LRP1 receptor, we investigated *in silico* also the interaction of the p.R1205H pathogenic variant modeled in complex with LRP1.<sup>33</sup> The results showed even more favorable energetics of this interaction compared to the p.P1127S variant ( $\Delta G = -15.7$  kcal/mol,  $K_d$  at  $25^\circ\text{C} = 3.10 \times 10^{-12}$  M; see Figure S4). By contrast, as a further validation, we investigated *in silico* the interaction between the benign VWF variant p.V1129G (3686T>G, D3 domain)<sup>34</sup> with cluster IV of LRP1. No significant variation of the binding energy compared to WT VWF was found ( $\Delta G = -13.9$  kcal/mol ( $K_d$  at  $25^\circ\text{C} = 6.48 \times 10^{-11}$  M), in agreement with the reported normal level and multimer profile of this variant.<sup>34</sup>

### 3.9 | Binding of VWF recombinant mutants to immobilized rLRP1-cIV/Fc

*In silico* findings were qualitatively validated by experimental evidence concerning the binding of both WT- and p.P1127S-VWF

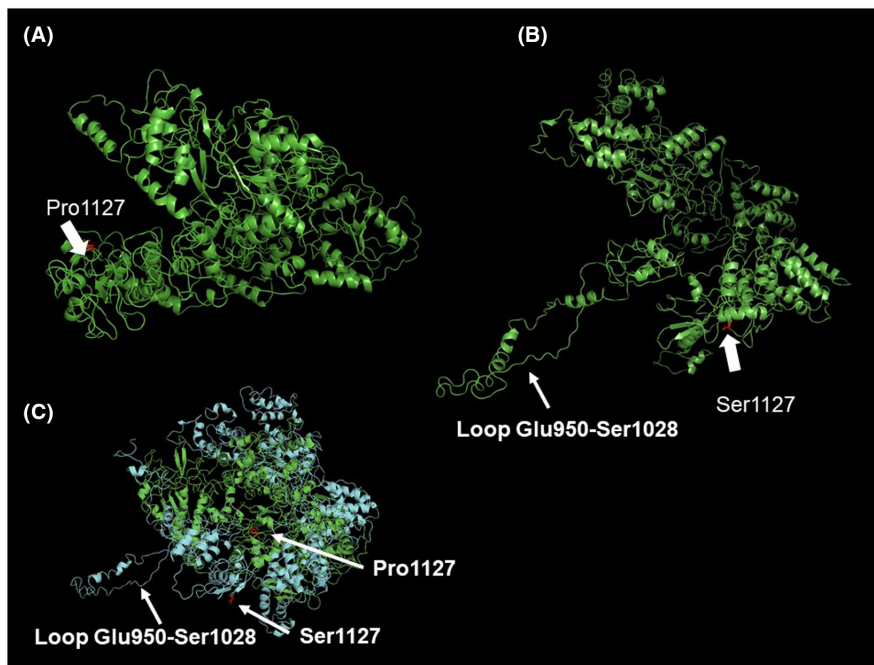


**FIGURE 4** Prediction of the molecular structure of the von Willebrand factor (VWF) sequence 764–2191 for both the wild-type (WT) (A) and the p.P1127S mutant (B). Model joining was performed by constraining the intra-chain disulfide bonds previously assigned with X-ray diffraction and biochemical studies.<sup>44</sup> The accuracy of the generated models was assessed with ResQ program,<sup>45</sup> which checks the residue-specific local quality of the I-TASSER models. ResQ algorithm analyzes and assessed the validity of several parameters: (A) the structural variations of Monte Carlo assembly simulations, (B) distance deviations of the templates detected by threading and structural alignment, (C) the threading alignment coverage, and (D) the consistency between the model and the sequence-based predictions of structural features. All structural analysis and image rendering were performed with the Pymol software (v. 2.3.3). The two models are shown in the same orientation. C, 3D alignment of the WT (green) and p.P1127S mutant (cyan). The side chain of both P1127 and S1127 are shown in red sticks. Pymol software was used to view and align the Protein Data Bank files generated by the I-TASSER and ResQ programs.

recombinant mutants to immobilized rLRP1-cIV/Fc. The WT form was characterized by a  $K_d$  value =  $0.65 \pm 0.1$  nM, whereas the heterozygous p.P1127S mutant bound to LRP1 with a  $K_d = 0.44 \pm 0.05$  nM, and the homozygous variant with a  $K_d = 0.18 \pm 0.03$  nM (Figure 7). A one-way analysis of variance showed that the three equilibrium binding constants were significantly different ( $p = .0316$ ,  $F = 5.195$ ,  $R^2 = .5358$ ) with an affinity magnitude ranking: *homozygous* > *heterozygous* > *WT*.

## 4 | DISCUSSION

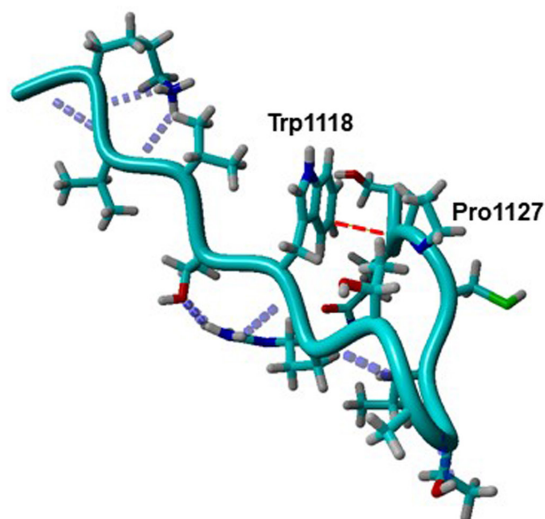
The phenotype associated with rare polymorphisms of proteins is often difficult to define, particularly in the heterozygous condition. To our knowledge, this is the first report on the phenotype associated to the heterozygous natural VWF p.P1127S variant (rs139579968). In accordance with the report of a rare VWF gene variant, the p.P1127S-VWF in the heterozygous form was associated with mild clinical manifestations. An apparent discordance was observed in the mother of the index case, who, although having the same VWF gene abnormality, showed higher VWF:Ag, VWF:GpIbR, and VWF:CBA levels. However, we should consider the age difference between the two subjects, differing by 30 years (see Table 1), knowing that in healthy subjects VWF level increases as a function

of age by as much as 15–17U/dl per decade.<sup>35,36</sup> The tendency of VWF to increase as a function of age was observed particularly in type 1 VWD,<sup>36,37</sup> especially in clinically milder disease forms. Besides the low VWF levels of the index case, the results pertaining to the clearance of VWF after desmopressin infusion in the index case deserved a plausible explanation. Hence, we investigated the molecular genetics of some relevant VWF scavenger receptors. An increasing number of cell surface receptors have been implicated in modulating the clearance of the VWF/FVIII complex. Based on this hypothesis, and with the limitation of genotyping in single subjects, we have investigated several SNVs in scavenger. Whereas identical genotypes were found in the index case and her mother for most polymorphisms, the index case was homozygous for the ASGR2 rs2289645 non-reference C allele whereas her mother was heterozygous. While evidence exists that ASGPR (ASGR1 and ASGR2 gene products) binds to and clears desialylated VWF, the evidence that ASGR2 contributes to the clearance of plasma-derived VWF in humans is more limited. Interestingly, in hemophilia A patients, the ASGR2 rs2289645 T > C genotypes were found to contribute, independently from and together with ABO blood groups, to the FVIII half-life.<sup>20</sup> Further, the CC genotype may predict in non-O blood group subjects lower FVIII levels (F.B, Francesco Bernardi unpublished results). Although ASGR2 genotype difference may contribute to develop additional hypotheses to explain differences in VWF



(A)

**Gly1115-Arg1133  
peptide sequence  
(WT)**



(B)

**Gly1115-Arg1133  
peptide sequence  
(p.P1127S)**

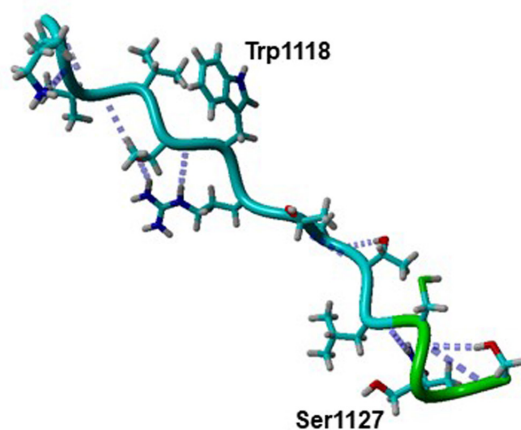


**FIGURE 5** Predicted 3D models of Gly1115-Arg1133 peptide sequence of wild-type (WT; A) and p.P1127S von Willebrand factor (VWF) mutant (B). The dotted lines represent intra-molecule hydrogen bonds. The dashed red line indicates the van der Waals contact between W1118 and P1127 in the WT form.

levels between family members in this study, the attribution of this variant as being a significant contributor to the low VWF phenotype of the patient is not supported by sufficient evidence. Further studies on a population level, including the interaction of age with ASGR2 gene variation, are needed.

The substitution of p.Pro1127 occurs in the exon 25 of the VWF molecule, where only a few natural mutations were reported in the European Association for Haemophilia and Allied Disorders Coagulation Factor Variant Database for VWF.<sup>38-40</sup> In the heterozygous form, the p.P1127S variant is associated with a mild clinical phenotype. Notably, the response to desmopressin was apparently normal in the index case, who showed a VWF level almost 3-fold higher after 1-h desmopressin infusion, as reported in [Table 1](#). However, we should not forget that the VWF clearance is a dynamic process, whereby the rate of VWF secretion is counterbalanced by its clearance driven by the VWF interaction with its scavenger receptors. Thus, is this the mechanism responsible for the reduced plasma level of this VWF variant? First, experimental evidence ruled out the possibility that an abnormal interaction with ADAMTS-13 or even elevated levels of the metalloprotease might cause an enhanced clearance of this VWF variant (see [Table 1](#) and [Figure S3](#)). Hence, we explored the hypothesis that, although in a heterozygous form, the pathogenic variant alters the conformation of the protein,

and favors its interaction with any scavenger receptors.<sup>18,41</sup> In silico docking simulations, performed using robust algorithms, were in accordance with this hypothesis and showed evidence of a different structural and energetic interaction between LRP1-VWF WT and LRP1-VWF variant. The latter, compared to WT-VWF, would employ different regions for binding to the cluster IV of the receptor ([Figure 6A,B](#)). Hence, the energetics of these interactions showed a better profile for the mutant than the WT form. The hypothesis was also supported by coherent docking simulations on prototypical pathogenic and benign variants. We cannot exclude that additional scavenging pathways of VWF<sup>41</sup> may have abnormal interaction with the p.P1127S mutant, thus accelerating the clearance of this mutant. Although the molecular mechanisms through which multimeric VWF interacts with the large LRP1 receptor remain poorly understood, our observations contribute mutation-based mechanisms and hypotheses. Whereas the p.R1306Q and p.V1316M pathogenic variants, previously shown to enhance VWF clearance via an LRP1-dependent mechanism,<sup>14</sup> are located within the A1 domain, we report that the p.P1127S missense variant in the D'D3 domain may produce a similar phenotype. Our findings are in accordance with in vitro studies suggesting that additional domains of VWF (D'D3 and D4) may contribute to LRP1 binding.<sup>42</sup> Of note, several studies have reported that even benign variants in the LRP1 gene, such as the

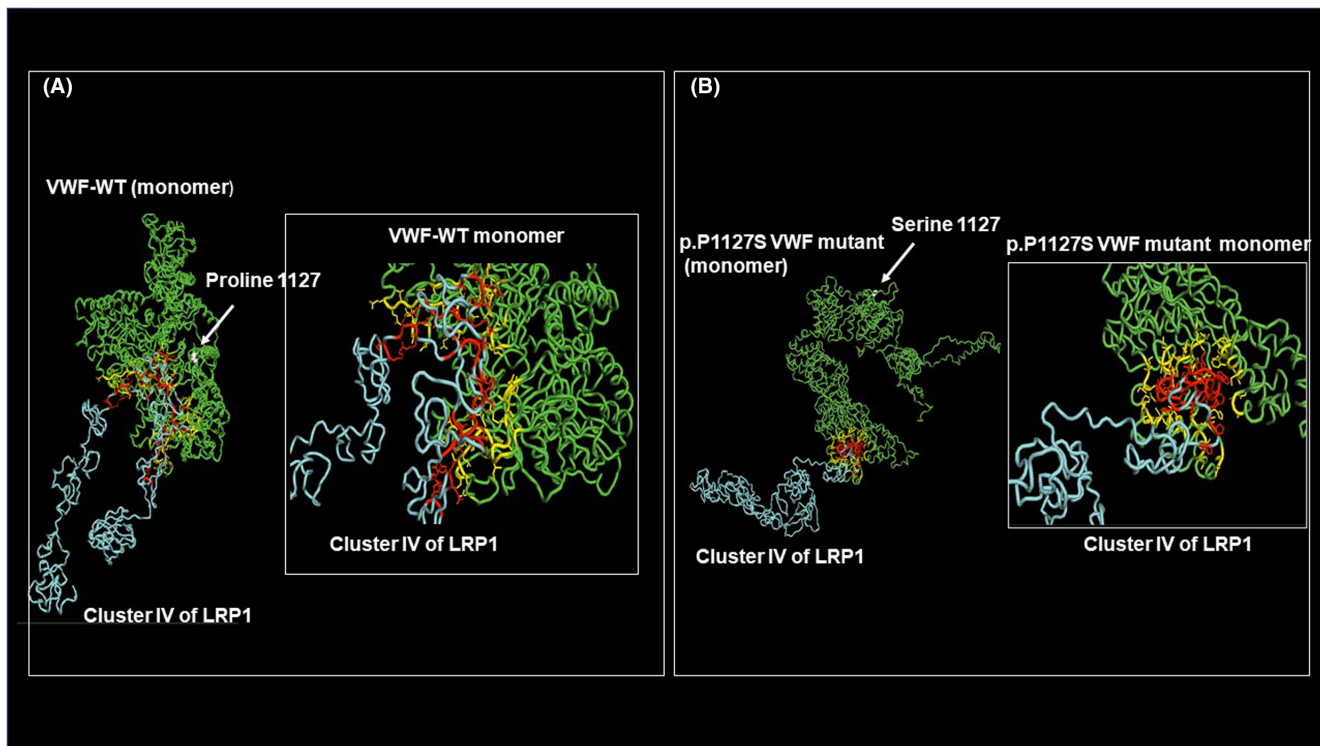


**FIGURE 6** A, Minimized *in silico* model of human lipoprotein receptor-related protein 1 (LRP1) Cluster IV complex with wild-type von Willebrand factor (WT-VWF) monomer and (B) p.P1127S VWF monomer. In the molecular modeling procedure, the disulfide bonds of the LRP1 domain were assigned employing the three-dimensional structure of a cysteine-rich repeat from the low-density lipoprotein receptor, showing a sequence analogy with the domain of LRP1 (Protein Data Bank code “1LDL”).<sup>46</sup> The docking of both WT and p.P1127S VWF monomer models with the final model of the LRP1 molecule was accomplished with the program SwarmDock server.<sup>47</sup> SwarmDock employs a protein-protein docking algorithm based on particle swarm optimization and was developed for flexible docking using normal modes as a method of modeling conformational change.<sup>48</sup> The energetics of the models concerning the adducts between LRP1 and both the WT-VWF and the p.P1127S forms was calculated with Prodigy server (<https://wenmr.science.uu.nl/prodigy/>).<sup>32</sup> On the right, a magnification of the interface region is also shown. The side chains of the LRP1 receptor (cluster IV) are shown in red sticks, whereas the interacting side chains of the p.1127S mutant are shown in yellow. The side chain of P1127 is shown as gray balls. Image rendering was performed with PyMOL software (version 2.1.1)

p.D2080N, can positively modulate the scavenger receptor activity and are associated with reduced levels of FVIII and VWF:Ag even in heterozygous individuals.<sup>43</sup> We must outline that the homozygous variant construct mostly showed *in vitro* a significantly higher affinity for LRP1, whereas the heterozygous construct showed just a milder although significant increase of affinity. However, in mild forms of type 1 VWD and likely in the low VWF disease, the effect of age may abolish or significantly reduce the initial reduction of VWF level. The results of the molecular modeling showed that the p.P1127S pathogenic variant causes a local disruption of the correct folding of the Gly1115-Arg1133 region. Proline is an amino acid larger than serine, with its side chain covalently bonded to the peptide backbone. This arrangement generates a closed ring system that restricts the peptide backbone to a limited area of conformational space. By contrast, the smaller serine residue, with just a two-atom side chain, allows greater peptide backbone conformational accessibility. *In silico* modeling reveals that the P1127S substitution results in the loss of multiple van der Waals contacts, including all to the W1118 residue (Figure 5). The conformational and thermodynamic effects of the loss of these contacts are clearly unfavorable and

are exacerbated by the placement of a polar atom. The loss of the hairpin-like conformation of this WT region causes long-distance effects on the conformation of the VWF monomer, propagating up to the Glu950-Ser1028 loop, which becomes more exposed to solvent and likely more flexible, as shown in Figure 4. This conformational transition seems to not affect the multimerization process, as experimentally demonstrated (Figure 1). However, the circulating VWF would spend shorter time in the circulation, as shown by PK analysis of the VWF profile after desmopressin infusion and by the modest but significant increase of the VWF:pp/VWF:Ag ratio after desmopressin infusion. Hence, additional mechanisms should be invoked to explain the significantly reduced half-life *in vivo* of this pathogenic variant.

This is a unique phenomenon for congenital bleeding disorders, whereby the diagnosis of type 1 VWD and low VWF disease could be ignored or rejected in older age, when the VWF level can reach normal values. Based on the case described in this study, it should be more advisable to take therapeutic decisions based on current VWF levels of the patients and consider their real hemorrhagic risk profile. Prospective studies on both healthy subjects and those with type

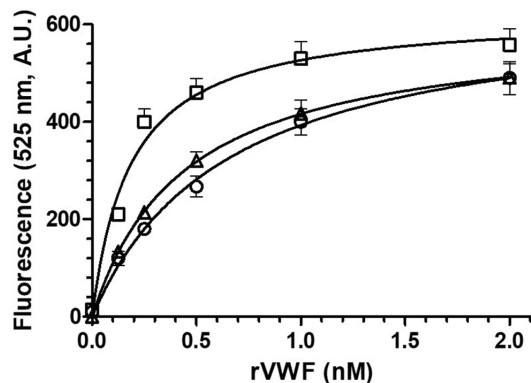


**FIGURE 7** Binding of wild-type (WT)- (O) and both heterozygous ( $\Delta$ ) and homozygous p.P1127S-VWF (von Willebrand factor;  $\square$ ) to immobilized human recombinant lipoprotein receptor-related protein 1 (rLRP1)-cIV/Fc. The continuous lines were drawn according to a single-site binding isotherm using the best-fit parameter values: Fluor(max) =  $650 \pm 42$  and  $K_d = 0.65 \pm 0.1$  nM for the WT form, Fluor(max) =  $601 \pm 25$  and  $K_d = 0.44 \pm 0.05$  nM for the heterozygous p.P1127S mutant, and Fluor(max) =  $624 \pm 31$  and  $K_d = 0.18 \pm 0.03$  nM for the homozygous p.P1127S mutant. The vertical bars are the standard error from two different measures. A one-way analysis of variance showed that the three equilibrium binding constants were significantly different ( $p = .0316$ ,  $F = 5.195$ ,  $R^2 = .5358$ ). The image rendering was obtained with the GraphPad software

1 VWD and low VWF phenotype are needed to address this issue and provide a validated cut-off range of VWF levels as a function of age, blood group, and possibly the PK profile of VWF levels after desmopressin treatment.

#### AUTHOR CONTRIBUTIONS

M. Sacco, A. Branchini, M. Tardugno, B. Giusti, M.F. Testa, B. Lunghi, and S. Lancellotti: performed the research and revised the manuscript. R. De Cristofaro: designed the research study, performed the MM studies, analyzed the data, and wrote the manuscript. G. Castaman: analyzed the data and critically revised the manuscript. F. Bernardi and M. Pinotti: analyzed the data and critically revised the manuscript.

#### ACKNOWLEDGMENTS

This work was supported by a grant from the Università Cattolica S. Cuore "Agostino Gemelli" - ROMA (Grant "Linea D1-2019").

#### CONFLICTS OF INTEREST

R. De Cristofaro has received honoraria for advisory board participation from Bayer, Sobi, and Takeda. G. Castaman has received honoraria for advisory board participation from Bayer, Roche, SOBI, CSL Behring, and Takeda. The remaining authors declare no interests that might be perceived as posing a conflict or bias.

#### ORCID

Monica Sacco  <https://orcid.org/0000-0002-2395-2691>

Alessio Branchini  <https://orcid.org/0000-0002-6113-2694>

Raimondo De Cristofaro  <https://orcid.org/0000-0002-8066-8849>

[org/0000-0002-8066-8849](https://orcid.org/0000-0002-8066-8849)

#### REFERENCES

- Meyer D, Girma JP. von Willebrand factor: structure and function. *Thromb Haemost.* 1993;70:99-104.
- Mancuso DJ, Tuley EA, Westfield LA, et al. Structure of the gene for human von Willebrand factor. *J Biol Chem.* 1989;264:19514-19527.
- Titani K, Kumar S, Takio K, et al. Amino acid sequence of human von Willebrand factor. *Biochemistry.* 1986;25:3171-3184.
- Sadler JE. Biochemistry and genetics of von Willebrand factor. *Annu Rev Biochem.* 1998;67:395-424.
- Keesler DA, Flood VH. Current issues in diagnosis and treatment of von Willebrand disease. *Res Pract Thromb Haemost.* 2017;2:34-41.
- Sadler JE, Budde U, Eikenboom JC, et al. Update on the pathophysiology and classification of von Willebrand disease: a report of the Subcommittee on von Willebrand Factor. *J Thromb Haemost.* 2006;4:2103-2114.
- Connell NT, Flood VH, Brignardello-Petersen R, et al. ASH ISTH NHF WFH 2021 guidelines on the management of von Willebrand disease. *Blood Adv.* 2021;5:301-325. doi:10.1182/bloodadvances.2020003264
- James PD, Connell NT, Ameer B, et al. ASH ISTH NHF WFH 2021 guidelines on the diagnosis of von Willebrand disease. *Blood Adv.* 2021;5:280-300. doi:10.1182/bloodadvances.2020003265
- Mazurier C, Meyer D. Factor VIII binding assay of von Willebrand factor and the diagnosis of type 2N von Willebrand disease - results of an international survey. On behalf of the Subcommittee on von Willebrand Factor of the Scientific and Standardization Committee of the ISTH. *Thromb Haemost.* 1996;76:270-274.
- Laffan MA, Lester W, O'Donnell JS, et al. The diagnosis and management of von Willebrand disease: a United Kingdom Haemophilia Centre Doctors Organization guideline approved by the British Committee for Standards in Haematology. *Br J Haematol.* 2014;167:453-465. doi:10.1111/bjh.13064
- Nichols WL, Hultin MB, James AH, et al. von Willebrand disease (VWD): evidence-based diagnosis and management guidelines, the National Heart, Lung, and Blood Institute (NHLBI) Expert Panel report (USA). *Haemophilia.* 2008;14:171-232. doi:10.1111/j.1365-2516.2007.01643.x
- Haberichter SL, Balistreri M, Christopherson P, et al. Assay of the von Willebrand factor (VWF) propeptide to identify patients with type 1 von Willebrand disease with decreased VWF survival. *Blood.* 2006;108:3344-3351. doi:10.1182/blood-2006-04-015065
- Haberichter SL, Castaman G, Budde U, et al. Identification of type 1 von Willebrand disease patients with reduced von Willebrand factor survival by assay of the VWF propeptide in the European study: molecular and clinical markers for the diagnosis and management of type 1 VWD (MCMDM-1VWD). *Blood.* 2008;111:4979-4985. doi:10.1182/blood-2007-09-110940
- Wohner N, Legendre P, Casari C, Christophe OD, Lenting PJ, Denis CV. Shear stress-independent binding of von Willebrand factor-type 2B mutants p.R1306Q & p.V1316M to LRP1 explains their increased clearance. *J Thromb Haemost.* 2015;13:815-820. doi:10.1111/jth.12885
- Lenting PJ, Van Schooten CJM, Denis CV. Clearance mechanisms of von Willebrand factor and factor VIII. *J Thromb Haemost.* 2007;5:1353-1360. doi:10.1111/j.1538-7836.2007.02572.x
- Lunghi B, Bernardi F, Martinelli N, et al. Functional polymorphisms in the LDLR and pharmacokinetics of Factor VIII concentrates. *J Thromb Haemost.* 2019;17:1288-1296. doi:10.1111/jth.14473
- Garcia-Martinez I, Borrás N, Martorell M, et al. Common genetic variants in ABO and CLEC4M modulate the pharmacokinetics

- of recombinant FVIII in severe hemophilia A patients. *Thromb Haemost.* 2020;120:1395-1406. doi:10.1055/s-0040-1714214
18. Swystun LL, Lai JD, Notley C, et al. The endothelial cell receptor stabilin-2 regulates VWF-FVIII complex half-life and immunogenicity. *J Clin Invest.* 2018;128:4057-4073. doi:10.1172/JCI96400
  19. Rastegarlarlari G, Pegon JN, Casari C, et al. Macrophage LRP1 contributes to the clearance of von Willebrand factor. *Blood.* 2012;119:2126-2134. doi:10.1182/blood-2011-08-373605
  20. Lunghi B, Morfini M, Martinelli N, et al. The asialoglycoprotein receptor minor subunit gene contributes to pharmacokinetics of factor VIII concentrates in hemophilia A. *Thromb Haemost.* 2021;75:45-48.
  21. Steirer LM, Park EI, Townsend RR, Baenziger JU. The asialoglycoprotein receptor regulates levels of plasma glycoproteins terminating with sialic acid alpha2,6-galactose. *J Biol Chem.* 2009;284:3777-3783. doi:10.1074/jbc.M808689200
  22. de Maistre E, Volot F, Mourey G, et al. Performance of two new automated assays for measuring von Willebrand activity: HemosIL AcuStar and Innovance. *Thromb Haemost.* 2014;112:825-830.
  23. Costa-Pinto J, Perez-Rodriguez A, Gómez-del-Castillo M d C, et al. Diagnosis of inherited von Willebrand disease: comparison of two methodologies and analysis of the discrepancies. *Haemophilia.* 2014;20:559-567.
  24. Veyradier A, Caron C, Ternisien C, et al. Validation of the first commercial ELISA for type 2N von Willebrand's disease diagnosis. *Haemophilia.* 2011;17:944-951.
  25. Lancellotti S, Peyvandi F, Pagliari MT, et al. The D173G mutation in ADAMTS-13 causes a severe form of congenital thrombotic thrombocytopenic purpura. A clinical, biochemical and in silico study. *Thromb Haemost.* 2016;115:51-62.
  26. Lancellotti S, De Filippis V, Pozzi N, et al. Formation of methionine sulfoxide by peroxynitrite at position 1606 of von Willebrand factor inhibits its cleavage by ADAMTS-13: a new prothrombotic mechanism in diseases associated with oxidative stress. *Free Radic Biol Med.* 2010;48:446-456. doi:10.1016/j.freeradbiomed.2009.11.020
  27. Lancellotti S, Dragani A, Ranalli P, et al. Qualitative and quantitative modifications of von Willebrand factor in patients with essential thrombocythemia and controlled platelet count. *J Thromb Haemost.* 2015;13:1226-1237. doi:10.1111/jth.12967
  28. Sacco M, Lancellotti S, Ferrarese M, et al. Noncanonical type 2B von Willebrand disease associated with mutations in the VWF D'D3 and D4 domains. *Blood Adv.* 2020;4:3405-3415. doi:10.1182/bloodadvances.2020002334
  29. Morling N, Allen RW, Carracedo A, et al. Paternity Testing Commission of the International Society of Forensic Genetics: recommendations on genetic investigations in paternity cases. *Forensic Sci Int.* 2002;129:148-157.
  30. Song J, Chen F, Campos M, et al. Quantitative influence of ABO blood groups on factor VIII and its ratio to von Willebrand factor, novel observations from an ARIC study of 11,673 subjects. *PLoS One.* 2015;10:e0132626. doi:10.1371/journal.pone.0132626
  31. Kozakov D, Hall DR, Xia B, et al. The ClusPro web server for protein-protein docking. *Nat Protoc.* 2017;12:255-278. doi:10.1038/nprot.2016.169
  32. Xue LC, Rodrigues JP, Kastriitis PL, Bonvin AM, Vangone A. PRODIGY: a web server for predicting the binding affinity of protein-protein complexes. *Bioinformatics.* 2016;32:3676-3678. doi:10.1093/bioinformatics/btw514
  33. Rawley O, O'Sullivan JM, Chion A, et al. von Willebrand factor arginine 1205 substitution results in accelerated macrophage-dependent clearance in vivo. *J Thromb Haemost.* 2015;13:821-826. doi:10.1111/jth.12875
  34. Bellissimo DB, Christopherson PA, Flood VH, et al. VWF mutations and new sequence variations identified in healthy controls are more frequent in the African-American population. *Blood.* 2012;119:2135-2140. doi:10.1182/blood-2011-10-384610
  35. Conlan MG, Folsom AR, Finch A, Davis CE, Sorlie P, Wu KK. Correlation of plasma protein C levels with cardiovascular risk factors in middle-aged adults: the Atherosclerosis Risk in Communities (ARIC) Study. *Thromb Haemost.* 1993;70:762-767.
  36. Rydz N, Grabell J, Lillicrap D, James PD. Changes in von Willebrand factor level and von Willebrand activity with age in type 1 von Willebrand disease. *Haemophilia.* 2015;21:636-641. doi:10.1111/hae.12664
  37. Borghi M, Guglielmini G, Mezzasoma AM, et al. Increase of von Willebrand factor with aging in type 1 von Willebrand disease: fact or fiction? *Haematologica.* 2017;102:e431-e433. doi:10.3324/haematol.2017.168013
  38. Goodeve A, Eikenboom J, Castaman G, et al. Phenotype and genotype of a cohort of families historically diagnosed with type 1 von Willebrand disease in the European study, Molecular and Clinical Markers for the Diagnosis and Management of Type 1 von Willebrand Disease (MCMDM-1VWD). *Blood.* 2007;109:112-121. doi:10.1182/blood-2006-05-020784
  39. James PD, Notley C, Hegadorn C, et al. The mutational spectrum of type 1 von Willebrand disease: results from a Canadian cohort study. *Blood.* 2007;109:145-154. doi:10.1182/blood-2006-05-021105
  40. Cumming A, Grundy P, Keeney S, et al. An investigation of the von Willebrand factor genotype in UK patients diagnosed to have type 1 von Willebrand disease. *Thromb Haemost.* 2006;96:630-641.
  41. O'Sullivan JM, Ward S, Lavin M, O'Donnell JS. von Willebrand factor clearance - biological mechanisms and clinical significance. *Br J Haematol.* 2018;183:185-195. doi:10.1111/bjh.15565
  42. Wohner N, Muczynski V, Mohamadi A, et al. Macrophage scavenger receptor SR-AI contributes to the clearance of von Willebrand factor. *Haematologica.* 2018;103:728-737. doi:10.3324/haematol.2017.175216
  43. Morange PE, Tregouet DA, Frere C, et al. Biological and genetic factors influencing plasma factor VIII levels in a healthy family population: results from the Stanislas cohort. *Br J Haematol.* 2005;128:91-99. doi:10.1111/j.1365-2141.2004.05275.x
  44. Zhou YF, Eng ET, Zhu J, Lu C, Walz T, Springer TA. Sequence and structure relationships within von Willebrand factor. *Blood.* 2012;120:449-458.
  45. Yang J, Wang Y, Zhang Y. ResQ: an approach to unified estimation of B-factor and residue-specific error in protein structure prediction. *J Mol Biol.* 2016;428:693-701.
  46. Daly NL, Scanlon MJ, Djordjevic JT, Kroon PA, Smith R. Three-dimensional structure of a cysteine-rich repeat from the low-density lipoprotein receptor. *Proc Natl Acad Sci U S A.* 1995;92:6334-6338. doi:10.1073/pnas.92.14.6334
  47. Torchala M, Bates PA. Predicting the structure of protein-protein complexes using the SwarmDock Web Server. *Methods Mol Biol.* 2014;1137:181-197. doi:10.1007/978-1-4939-0366-5\_13
  48. Torchala M, Moal IH, Chaleil RA, Agius R, Bates PA. A Markov-chain model description of binding funnels to enhance the ranking of docked solutions. *Proteins.* 2013;81:2143-2149. doi:10.1002/prot.24369

## SUPPORTING INFORMATION

Additional supporting information may be found in the online version of the article at the publisher's website.

**How to cite this article:** Sacco M, Lancellotti S, Branchini A, et al. The p.P1127S pathogenic variant lowers von Willebrand factor levels through higher affinity for the macrophagic scavenger receptor LRP1: Clinical phenotype and pathogenic mechanisms. *J Thromb Haemost.* 2022;20:1818-1829. doi: [10.1111/jth.15765](https://doi.org/10.1111/jth.15765)